

Communications

Production of Bulk Cementite and Its Characterization

M. UMEMOTO, Z.G. LIU, H. TAKAOKA,
M. SAWAKAMI, K. TSUCHIYA, and K. MASUYAMA

Bulk cementite has been synthesized through a combination of mechanical alloying (MA) and spark plasma sintering (SPS). A density of 98 pct of the theoretical value was reached. It is believed that this is a first report on synthesized bulk cementite. The main properties of bulk cementite have been measured, such as microhardness, compression properties, thermal expansion, thermoelectric properties, specific heat, etc. The successful synthesis of bulk cementite will enable more intensive investigation on cementite related alloys.

Cementite is one of the most important phases in steels, which plays a critical role in the mechanical properties of steels. As a basic phase in steels, the understanding of its mechanical, physical, and chemical properties is particularly desired. It is claimed to be metastable at all temperatures with respect to graphite and its saturated solution in iron.^[1] Its structure has been well studied and determined. Although it has been well known that cementite is harder than ferrite and is quite brittle,^[2] some reports claimed that cementite deforms plastically in drawn pearlitic steels during elevated temperature.^[3,4] However, the mechanical behavior of cementite is far from well understood.

So far, decades of effort have been devoted to understanding the mechanical properties of cementite in view of better controlling the mechanical properties of steels.^[5-12] Mechanical properties, such as hardness, Young's modulus, shear modulus, fracture toughness, and their composition and temperature dependence, are the most desired. Since the 1950s, several reports about mechanical properties of cementite have been published on the cementite in a ferrite matrix or electrolytically extracted from steels or cast iron.^[6-12] However, large errors were inevitable due to their small size as well as the effects of heat treatments. More recently, Mizubayashi, *et al.* have made some improvements on thin films of cementite.^[12] An electron-shower assisted physical vapor deposition (PVD) process was employed to prepare single-phase cementite films with a thickness of around 2.5 to 3.0 μm . Young's modulus, Poisson's ratio, and Vicker's hardness were measured, which resulted in similar data to the previous work that used other methods.

Nevertheless, until now, there have been few reports on the properties of bulk cementite; these are needed in order

to have more meaningful data to evaluate the properties of steels.

Our recent endeavor has led to successful fabrication of bulk cementite by MA with subsequent SPS. Although MA had been applied to the Fe-C system several years ago,^[13,14,15] the emphasis was not put on the synthesis of bulk cementite. Bulk cementite with dimensions of up to $\phi 15 \times 10$ mm has been produced in the present study. To our knowledge, this is the first produced bulk cementite. The basic mechanical and physical properties were measured and compared to the previous results of cementite produced by other methods. More intensive work on the effect of composition and of substitutional additions, such as Cr and Mn for Fe, is currently under way.

The starting materials were elemental powders of Fe and graphite with a purity and particle size of Fe: 99.9 pct and $<100 \mu\text{m}$, and C: 99.9 pct and $<5 \mu\text{m}$, respectively. The powders were mixed at compositions of 75 at. pct Fe and 25 at. pct C. Mechanical alloying was performed on a conventional horizontal ball mill with a ball-to-powder weight ratio of 100:1. The maximum milling time was 18,000 ks. All the milling was carried out under an argon atmosphere. The resultant powders were then subjected to x-ray diffraction (XRD) analysis for phase determination. Thermal analysis of the milled powders was monitored in a Rigaku Thermo Plus 2 DSC 8230L, (Rigaku Denki Co., Tokyo, Japan) differential scanning calorimeter (DSC) at a heating rate of 20 K/min up to 973 K under a flow of argon gas at 30 mL/min. Two continuous runs were carried out for the same sample, in which the first run was blanked by the second one to obtain the true DSC curve. Spark plasma sintering was used to produce compacts of the cementite.^[16] The sintering was carried out in vacuum under a pressure of 50 MPa for 300 seconds at various temperatures, in which 1173 K was finally chosen as optimal. The density of the obtained compacts was measured by the Archimedes method. Subsequently, optical microscope (Nikon ME600, Tokyo, Japan), scanning electron microscope (SEM, JEOL* JEM-6300), and trans-

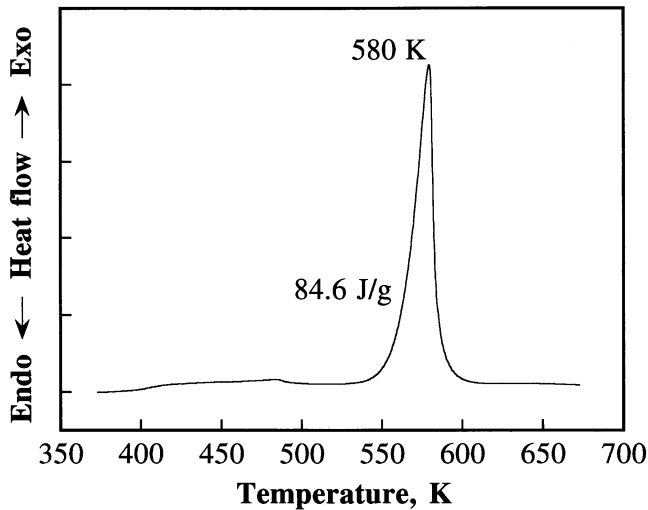
*JEOL is a trademark of Japan Electron Optics Ltd., Tokyo.

mission electron microscope (Hitachi H-800, Tokyo, Japan) were used for structural characterization. Compression tests were done in air using an Instron universal tester at a cross-head speed of 0.5 mm/min, at room temperature, 573 K, and 773 K. Hardness measurements were performed on an Akashi Co. (Tokyo, Japan) MVK-G1 micro-Vicker's hardness tester with a 0.98 N load for 15 s and on a Nikon QM high-temperature hardness tester. Thermal expansion was measured on a Fujidenpa (Saitama, Japan) Formaster-F tester. The electric conductivity and Seebeck coefficient were measured using a Shinku Rikou (Yokohama, Japan) ZEM-1 thermoelectric tester.

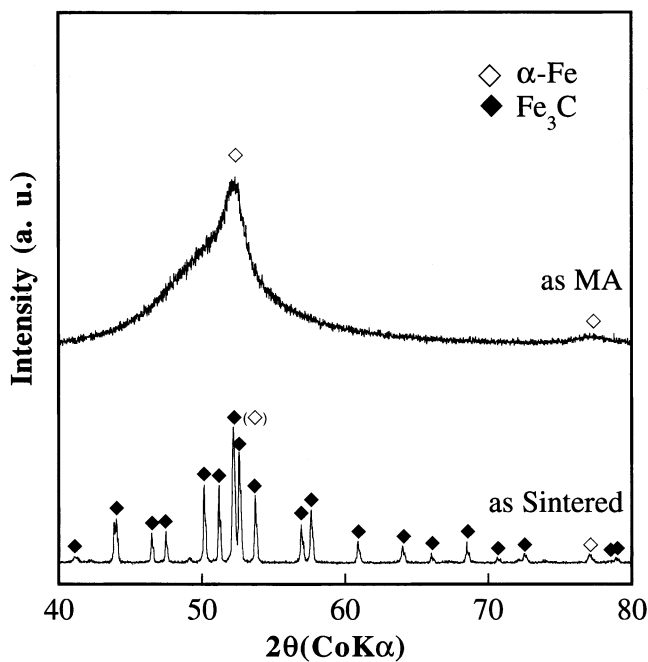
X-ray diffraction analysis was undertaken to monitor the structural evolution during MA. After 360 ks of milling of the 75Fe/25C powder mixture, a body-centered-cubic structure phase formed with a particle size of less than 5 μm . It was characterized as Fe-C mixture or, more possibly, $\alpha\text{-Fe(C)}$ solid solution. Longer milling time resulted in the formation of a carbide (Fe_7C_3 structure), which is harder and difficult to sinter. Thus, the powders milled for 360 ks were chosen to be investigated in the subsequent experiments.

M. UMEMOTO, Professor, Z.G. LIU, Research Associate, H. TAKAOKA and M. SAWAKAMI, Graduate Students, and K. TSUCHIYA, Associate Professor, are with the Department of Production Systems Engineering, Toyohashi University of Technology, Toyohashi 441-8580, Japan. K. MASUYAMA, Research Associate, is with the Department of Mechanical Engineering, Toyama National College of Technology, Toyama 939, Japan.

Manuscript submitted September 19, 2000.



(a)



(b)

Fig. 1—(a) DSC curve of as-milled 75Fe/25C powder. (b) XRD patterns of as-milled and as-aged 75Fe/25C powder.

The DSC analysis of the milled powders revealed an exothermic reaction at a temperature of 580 K (Figure 1(a)), which was determined by XRD to be the formation reaction of cementite Fe₃C (Figure 1(b)). This result corresponds well with that reported previously.^[13] The DSC measurements were repeated many times to determine precisely the heat release of carbide formation. The measured heat release scattered from 73.6 to 105.6 J/g due to the complicated structure at as-milled state. Figure 1(a) shows an example with a heat release of 84.6 J/g. A heat release of 100 J/g was obtained by extrapolating from the dual-phase structure of α-Fe + Fe₃C. Therefore, the heat release was calculated to be about 18 kJ/mol for one mole Fe₃C (179 g/mol). This value corresponds to the enthalpy difference between the as-milled mixture of 3Fe + C and cementite (Fe₃C) and

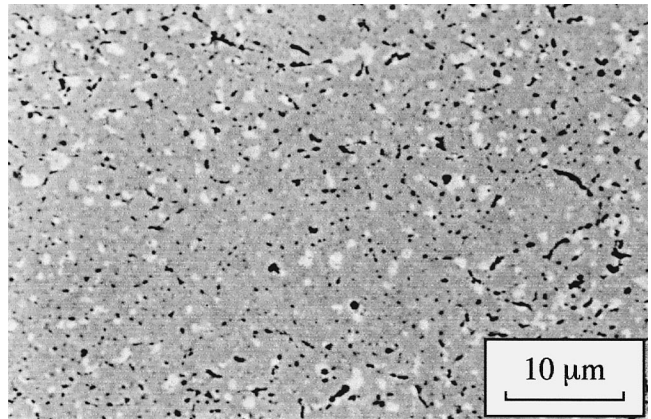


Fig. 2—SEM micrograph of the cross section of the sintered cementite compact.

does not correspond to the formation heat of cementite from iron and graphite (about -30 kJ/mol^[17]). Mechanical milling raised the enthalpy of the 75Fe/25C mixture mainly by the grain refinement of graphite powder and partly by the dissolution of carbon into iron and the nanocrystallization of iron, as will be discussed later.

The as-milled powders were subsequently sintered by SPS at 1173 K. Though the XRD pattern in Figure 1(b) revealed only peaks attributed to the cementite, there existed a possibly minor amount of other phases, such as ferrite and graphite, formed by the decomposition of cementite in the sintering process. It appears that the applied external pressure suppresses the decomposition of the cementite upon heating, since the molar volume of cementite is smaller than that of the corresponding amount of iron and graphite. The volume difference ΔV between Fe₃C and three moles of Fe and one mole of graphite is about -3 cm³. The pressure applied (50 MPa) during sintering stabilizes cementite with respect to the elemental mixture of 75Fe/25C by about 40 J/g·atom. At around the sintering temperature (1173 K), this stabilizing effect by pressure is about 30 pct of the driving force for the decomposition of cementite (140 J/g·atom at 1173 K obtained by THERMO-CALC).

Figure 2 shows a SEM micrograph of a sintered cementite compact after etching. The observed voids had a diameter of less than 0.5 μm. Some black spots and white spots were attributed to graphite and iron, respectively, which are considered to be less than 5 vol pct. The sintered cementite compact had a measured relative density of 98 pct. The polished surface had a metallic glare like iron.

Microhardness of the cementite bulk was measured to be as high as 1000 HV. The previously reported hardness of cementite scattered in a wide range. The early study on a hypereutectoid steel (1.2 pct C) reported a microhardness about 1270 HV of primary cementite.^[18] The recent study on a hypereutectic cast iron revealed a hardness of 988 HV in the eutectic cementite and 1370 HV in the primary cementite.^[10] A more recent study on cementite film reported a microhardness of 1230 HV.^[19] Apparently, the previous results were affected by the starting composition, microstructure, and subsequent treatments (even the load in the test may exert an influence to the final results). Compared with those values, the present value is somehow low due to the lower density and the existence of voids and α-Fe.

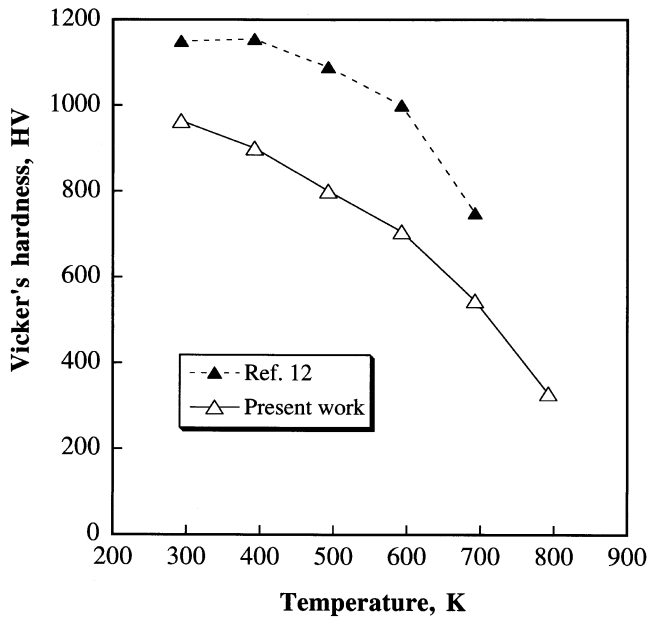


Fig. 3—Tested Vickers hardness vs temperature. Load, 0.98 N; and loading time, 15 s. In reference, load, 0.0245 N; and film thickness, 3 μm .

A temperature dependence of hardness was measured for the cementite compact (Figure 3). With increasing temperature, the hardness of the samples decreased from above 1000 HV at room temperature to around 330 HV at 773 K. The higher the temperature, the greater the decrease. This phenomenon is believed to relate with creep. A similar effect of temperature on hardness has been reported in testing of thin film cementite with a thickness of 2.5 to 3.0 μm ,^[12] although the loads in the two tests were different. The higher hardness values in the reference may be attributed to the smaller load on the thin film, for which the dependence of hardness on loads is very strong.^[20]

The compression test was carried out to characterize the mechanical properties of cementite. Samples with dimensions of 4 \times 4 \times 6 mm were cut from the sintered cementite compact and were ground and polished to a 0.05- μm alumina finish. Figure 4 shows the compression strengths of the cementite specimens at three different temperatures. The samples at room temperature and 573 K revealed similar maximum stresses of 2.61 and 2.59 GPa, respectively, without any detectable plastic deformation. However, at higher temperature (773 K), a drastic decrease of maximum stress down to 1.39 GPa was observed along with a plastic deformation as large as 10 pct, which was obtained prior to fracture. The room-temperature fracture stress of proeutectoid cementite ribbon extracted from carbon steel was measured by a bending test to be 4 to 8 GPa.^[5] This large scatter is due to the small specimen size tested (1- to 3- μm thick and 1-mm long). Therefore, no reliable data on mechanical properties of cementite by tension, compression, or bending tests have been reported thus far.

Figure 5 shows the thermal expansion curve of cementite between 373 to 773 K. It reveals thermal expansion coefficients of 7.6 K^{-1} at 373 K, 16.5 K^{-1} at 573 K, and 16.9 K^{-1} at 673 K respectively. An apparent kink on the thermal expansion diagram at the Curie temperature of cementite

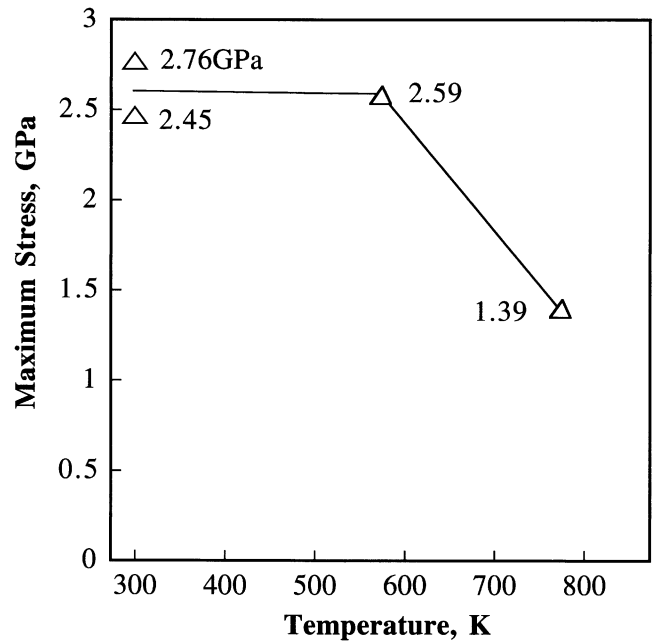


Fig. 4—Maximum compression strength of bulk cementite as a function of temperature. Strain rate: $2.14 \times 10^{-3} \text{ s}^{-1}$. No plastic deformation was observed for samples tested at 300 and 573 K.

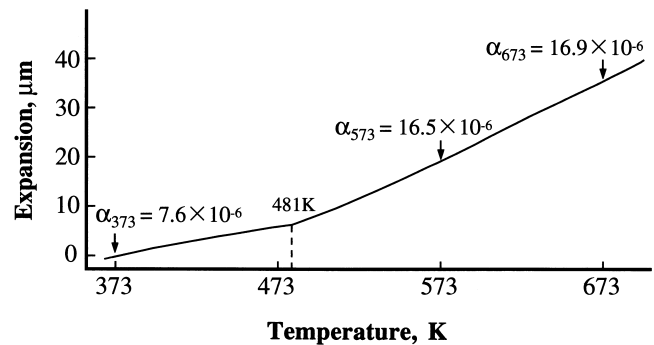


Fig. 5—Thermal expansion curve of bulk cementite (MA for 100 h, and sintered at 1173 K, 50 MPa, 300 s). The average coefficients are indicated on the curve.

appears (481 K). The average thermal expansion coefficient was calculated to be $1.62 \times 10^{-5} \text{ K}^{-1}$ for 481 to 773 K (above the Curie temperature) and $6.8 \times 10^{-6} \text{ K}^{-1}$ for 373 to 481 K (below the Curie temperature), respectively. The latter is much smaller compared with that of pure iron within the same temperature range. This smaller thermal expansion coefficient just below T_c is induced by magnetostriction in the cementite.^[7,21,22] In the literature, the thermal expansion coefficient of cementite was either estimated from the extrapolated data of the cast iron or obtained from electrolytically extracted cementite by either dilatometry or XRD. Some values are in the same magnitude with the present measurements, *e.g.*, $\sim 2 \times 10^{-5} \text{ K}^{-1}$ above T_c (derived from Figure 4 in Reference 21). The decomposition of cementite into α -Fe and graphite was observed above 853 K in the present study, detected by the change of thermal expansion, electrical resistivity, and XRD structural observation.

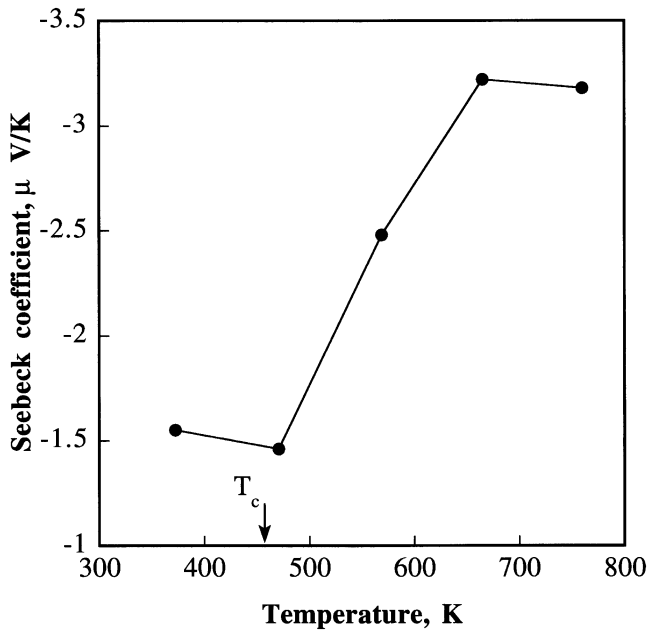


Fig. 6—Seebeck coefficient of bulk cementite (MA for 100 h, and sintered at 1173 K, 50 MPa, 300 s) vs temperature.

The Seebeck coefficient has also been measured for the present bulk cementite, which is shown in Figure 6. Negative Seebeck values were obtained, indicating an *n*-type thermoelectric effect. At temperatures below the Curie temperature, it was measured to be around $-1.5 \mu\text{V/K}$, increasing linearly with increasing temperature up to 673 K from -1.46 $-3.22 \mu\text{V/K}$. However, when the temperature was increased to above 773 K, the values started to decrease due to the possible decomposition of cementite, as such a change was observed in the thermal expansion measurements at the same temperature.

Specific heat of bulk cementite was also measured. The measurements revealed a specific heat of $106.1 \text{ J/mol}\cdot\text{K}$ at 373 K for the present bulk cementite. This value is quite close to the reported room-temperature specific heat of cementite of $106.6 \text{ J/mol}\cdot\text{K}$.^[23]

The measured electric conductivity of the bulk cementite is represented in Figure 7. As with many metallic materials, it was found that the electric conductivity decreases slightly but linearly with increasing temperature, and was $12.7 \times 10^3 \Omega/\text{cm}$ at 373 K. A slight decrease of electric conductivity was found with temperature up to 853 K. In contrast, the electric conductivity for pure iron^[24] decreases significantly with increasing temperature, which is also shown in Figure 7.

The formation of metastable cementite from stable iron and graphite mixture by ball milling can be considered as follows. Mechanical milling resulted in grain refinement of both iron and graphite, and probably solid solution of carbon atoms in the iron matrix, which increases the energy level of the milled powders to higher than that of cementite (Fe_3C). The enthalpy of cementite ($1/4\text{Fe}_3\text{C}$) is $8.9 \text{ kJ/g}\cdot\text{atom}$ higher than that of the mixture of $75\text{Fe}(\alpha)/25\text{C}(\text{graphite})$ at 580 K.^[17] The heat release in the formation reaction measured by DSC of the milled $75\text{Fe}/25\text{C}$ powder is 4.5 kJ for $1/4\text{Fe}_3\text{C}$. Thus, the enthalpy of MA

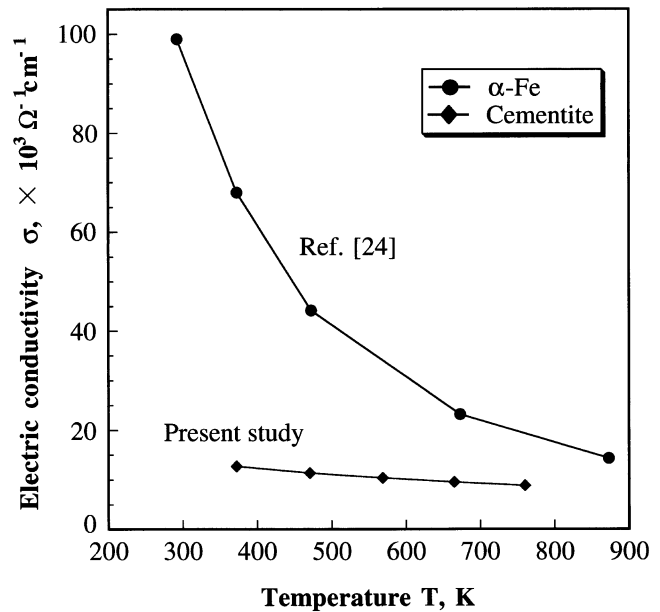


Fig. 7—Electric conductivity of bulk cementite (MA for 100 h, and sintered at 1173 K, 50 MPa, 300 s) vs temperature. The values of pure iron are shown for comparison.

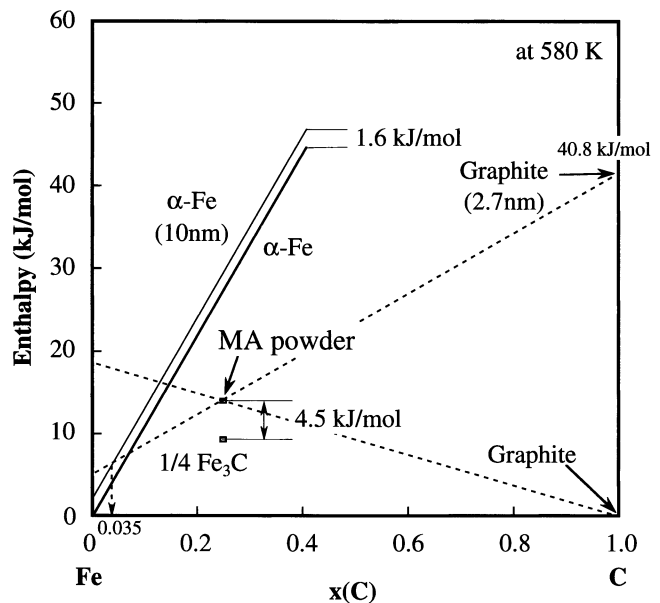


Fig. 8—Energy consideration of the formation of cementite from mechanically alloyed iron and graphite elemental powders.

powder is 13.4 kJ higher than the mixture of $75\text{Fe}(\alpha)/25\text{C}(\text{graphite})$. The particle size refinement of graphite by ball milling was reported by Nagano *et al.*^[25] The estimated graphite diameter of 2.7 nm after ball milling gives the increase in enthalpy by $40.8 \text{ kJ/g}\cdot\text{atom}$. Nanocrystallization (10 nm) of Fe results in an increase in enthalpy by $1.6 \text{ kJ/g}\cdot\text{atom}$. Taking these into account, Figure 8 predicts a 3.5 at. pct carbon content in Fe. Although this solution value is slightly larger than the estimated value of about 1 at. pct from lattice expansion, the preceding calculation

explains the importance of the graphite particle size refinement by ball milling for the formation of Fe₃C.

As a brief summary, the bulk cementite has been fabricated through the combination of mechanical alloying of Fe and C powder mixtures and the subsequent sintering. The microstructure, mechanical, and physical properties of bulk cementite have been characterized as well. It is believed that this is the first to produce and characterize bulk cementite. The present result will be beneficial to further research work on cementite and on the improvement of understanding the structure and properties of steels.

ACKNOWLEDGMENTS

This work is partly supported by the Ferrous Super Metal Consortium of Japan under the auspices of NEDO and by the Strategic Research Project of Iron and Steel Institute of Japan. The authors express their gratitude to Professor Y. Tomota, Ibaraki University, for carrying out the compression test.

REFERENCES

1. L.S. Darken and R.W. Gurry: *AIME Trans.*, 1951, pp. 1015-18
2. H.E. McGannon: *The Making, Shaping and Treating of Steel*, U.S. Steel Co., Pittsburgh, PA, 1971, p. 1077.
3. A. Inoue, T. Ogura, and T. Masumoto: *Trans. JIM*, 1976, vol. 17, pp. 149-57.
4. A.A. Bataev, V.I. Tushinskii, and V.A. Bataev: *Phys. Met. Metall.*, 1995, vol. 80, pp. 580-84.
5. W.W. Webb and W.D. Forgeng: *Acta Metall.*, 1958, vol. 6, pp. 462-69.
6. B.M. Drapkin and B.V. Fokin: *Phys. Met. Metall.*, 1980, vol. 49, pp. 177-80.
7. A. Kagawa, T. Okamoto, and H. Matsumoto: *Acta Metall.*, 1987, vol. 35, pp. 797-803.
8. A.P. Miodownik: *Mater. Sci. Technol.*, 1994, vol. 10, pp. 190-92.
9. S. Hartmann and H. Ruppertsberg: *Mater. Sci. Eng. A*, 1995, vol. 190, pp. 231-39.
10. B.M. Drapkin, G.M. Kimstach, and T.D. Molodtsova: *Met. Sci. Heat Treatment*, 1996, vol. 38, pp. 408-09.
11. T.J. Goodwin, S.H. Yoo, P. Matteazzi, and J.R. Groza: *Nanostruct. Mater.*, 1997, vol. 8, pp. 559-66.
12. H. Mizubayashi, S.J. Li, H. Yumoto, and M. Shimotomai: *Scripta Mater.*, 1999, vol. 40, pp. 773-77.
13. T. Tanaka, S. Nasu, K. Nakagawa, K.N. Ishihara, and P.H. Shingu: *Mater. Sci. Forum*, 1992, vols. 88-90, pp. 269-74.
14. G. Le Caer, E. Bauer-Grosses, A. Pianelli, E. Bouzy, and P. Matteazzi: *J. Mater. Sci.*, 1990, vol. 25, pp. 4726-31.
15. S.J. Campbell, G.M. Wang, A. Calka, and W.A. Kaczmarek: *Mater. Sci. Eng. A*, 1997, vol. 226-228, pp. 75-79.
16. M. Tokita: *J. Soc. Powder Technol. Jpn.*, 1993, vol. 30, pp. 790-804.
17. J. Chipman: *Metall. Trans.*, 1972, vol. 3, pp. 55-64.
18. A. Inoue, T. Ogura, and T. Masumoto: *Bull. Jpn. Inst. Met.*, 1974, vol. 13, p. 653.
19. S.J. Li, M. Ishihara, H. Yumoto, T. Aizawa, and M. Shimotomai: *Thin Solid Films*, 1998, vol. 316, pp. 100-04.
20. Z.G. Liu, K. Tsuchiya, and M. Umemoto: Toyohashi University of Technology, Toyohashi, unpublished research, 2000.
21. A. Kagawa and T. Okamoto: *Trans. JIM*, 1979, vol. 20, pp. 659-66.
22. A. Kagawa and T. Okamoto: *J. Mater. Sci.*, 1983, vol. 18, pp. 225-30.
23. Kosolapova: *Carbides*, Plenum Press, New York, NY, 1971, p. 29.
24. *Metals Reference Book*, 5th ed., Butterworth and Co., London, 1976.
25. K. Nagano, H. Wakayama, Y. Fukushima, T. Fukunaga, and U. Mizutani: *J. Jpn. Soc. Powder Metall.*, 1996, vol. 43, pp. 738-41.

Discussion of "The Role of Manganese and Copper in the Eutectoid Transformation of Spheroidal Graphite Cast Iron"*

OSCAR MARCELO SUAREZ and CARL R. LOPER Jr.

A few comments should be made concerning the effect of Mn and Cu in the solid-state transformation of nodular iron discussed by Lacaze *et al.*^[1] The eutectoid transformation of several cast irons and Si steels was studied using the differential thermal analysis (DTA) method at different cooling rates. These DTA results were contrasted with thermodynamic modeling of the corresponding Fe-C-Si metastable and stable equilibrium phase diagram. Since the bulk of the investigation of the writers of this discussion relates to ferritic ductile irons,^[2,3] only the stable phase diagram analyzed by Lacaze *et al.* will be discussed.

Figure 1 presents a schematic of an isopleth section of the stable Fe-C-Si phase diagram. The austenite (γ) + graphite (G) \leftrightarrow austenite (γ) + graphite (G) + ferrite (α) transformation temperature is designated T_{α}^0 , while T_{α} designates the $\gamma + G + \alpha \leftrightarrow G + \alpha$ transformation temperature. Therefore, under conditions approaching equilibrium, at temperatures equal to or just below T_{α}^0 , the onset of ferrite formation should be expected. This was neither the case in Lacaze *et al.*'s^[1] research nor in more recent investigations.^[3] Even at very low cooling rates from temperatures with little superheat above the predicted transformation temperatures, the alloys start forming ferrite at or below T_{α} in most cases. According to Lacaze *et al.*, carbon diffusion from parent austenite through the ferrite shell into the graphite nodule required that "the carbon content . . . at the ferrite/austenite interface must be higher than at the ferrite/graphite interface." Therefore, "this condition is fulfilled only at temperatures lower than the lowest temperature of the three-phase austenite/ferrite/graphite field," *i.e.*, T_{α} . In other words, based on kinetic considerations, the precondition for the formation of ferrite is that the alloy be at a temperature at or below the crossover of the lines e-f-d and f-b in Figure 1, *i.e.*, below T_{α} . This would explain the large undercoolings observed by Lacaze *et al.* and corroborated by the present researchers. In a train of thought later elaborated on by Linares *et al.*,^[3] the available driving force for the formation of ferrite at a given undercooling becomes the carbon concentration difference: $C_{\alpha/\gamma} - C_{\alpha/G}$, *i.e.*, the concentration along the α/γ boundary (line f-b in Figure 1) minus the concentration along the α/G boundary (line f-d in Figure 1) at a given temperature.

Using the same thermodynamic package as used by

*J. LACAZE, A. BOUDOT, V. GERVAL, D. OQUAB, and H. SANTOS: *Metall. Mater. Trans. A*, 1997, vol. 28A, pp. 2015-25.

OSCAR MARCELO SUAREZ, formerly Research Assistant, Department of Materials Science and Engineering, University of Wisconsin-Madison, is Assistant Professor, Department of General Engineering, University of Puerto Rico-Mayaguez, Mayaguez, Puerto Rico 00681. e-mail: msuarez@ece.uprm.edu. CARL R. LOPER, Jr., Professor, is with the Department of Materials Science and Engineering, University of Wisconsin-Madison, Madison, WI 53706.

Discussion submitted February 2, 2001.